A&A 585, A5 (2016)
DOI: 10.1051/0004-6361/201527297

Astronomy & Astrophysics

Age consistency between exoplanet hosts and field stars

A. Bonfanti[1,2], S. Ortolani[1,2], and V. Nascimbeni[2]

[1] Dipartimento di Fisica e Astronomia, Università degli Studi di Padova, Vicolo dell'Osservatorio 3, 35122 Padova, Italy
e-mail: andrea.bonfanti.1@studenti.unipd.it
[2] Osservatorio Astronomico di Padova, INAF, Vicolo dell'Osservatorio 5, 35122 Padova, Italy

Received 2 September 2015 / Accepted 3 November 2015

ABSTRACT

Context. Transiting planets around stars are discovered mostly through photometric surveys. Unlike radial velocity surveys, photometric surveys do not tend to target slow rotators, inactive or metal-rich stars. Nevertheless, we suspect that observational biases could also impact transiting-planet hosts.
Aims. This paper aims to evaluate how selection effects reflect on the evolutionary stage of both a limited sample of transiting-planet host stars (TPH) and a wider sample of planet-hosting stars detected through radial velocity analysis. Then, thanks to uniform derivation of stellar ages, a homogeneous comparison between exoplanet hosts and field star age distributions is developed.
Methods. Stellar parameters have been computed through our custom-developed isochrone placement algorithm, according to Padova evolutionary models. The notable aspects of our algorithm include the treatment of element diffusion, activity checks in terms of $\log R'_{HK}$ and $v \sin i$, and the evaluation of the stellar evolutionary speed in the Hertzsprung-Russel diagram in order to better constrain age. Working with TPH, the observational stellar mean density $\rho_\star$ allows us to compute stellar luminosity even if the distance is not available, by combining $\rho_\star$ with the spectroscopic $\log g$.
Results. The median value of the TPH ages is ~5 Gyr. Even if this sample is not very large, however the result is very similar to what we found for the sample of spectroscopic hosts, whose modal and median values are [3, 3.5) Gyr and ~4.8 Gyr, respectively. Thus, these stellar samples suffer almost the same selection effects. An analysis of MS stars of the solar neighbourhood belonging to the same spectral types bring to an age distribution similar to the previous ones and centered around solar age value. Therefore, the age of our Sun is consistent with the age distribution of solar neighbourhood stars with spectral types from late F to early K, regardless of whether they harbour planets or not. We considered the possibility that our selected samples are older than the average disc population.

Key words. stars: evolution – Hertzsprung-Russell and C-M diagrams – planetary systems

1. Introduction

Computing ages of field stars is very challenging because the age is not a direct observable. Thanks to models, information about the age comes from the composition and evolutionary state of the core of a star, while we are mostly limited to observing the properties at the surface. Several techniques can be applied.

Using the stellar effective temperature $T_{\rm eff}$ and luminosity L as input values, age can be computed through interpolation in the grids of isochrones (isochrone placement). Instead, gyrochronology (see e.g. Barnes & Kim 2010) is an empirical technique that allows the determination of stellar ages considering that the rotational speed of stars declines with time because of magnetic braking. Asteroseismology (see Handler 2013 for a review) is a very promising technique because the individual oscillation frequencies are directly linked to the inner density profile and the sound propagation speed in the stellar core. These frequencies are recovered through detailed analyses and high-precision photometry, which facilitates the determination of very precise, though model-dependent, ages. If it is not possible to investigate each oscillation mode, asteroseismic studies simply give global parameters i.e. the large frequency separation $\Delta\nu$ and the frequency of maximum power $\nu_{\rm max}$, which are linked to the stellar mean density $\rho_\star$ and surface gravity $\log g$ (see e.g. Kjeldsen & Bedding 1995). In this case, asteroseismology loses part of its strength. Input $T_{\rm eff}$, $\rho_\star$ and $\log g$ again require isochrones to compute ages as in Chaplin et al. (2014), however, asteroseismic $\log g$ is known with better precision if compared with the spectroscopic value, for instance. For a broad review about different age computation methods, see Soderblom (2010).

Since $T_{\rm eff}$ and L can be usually recovered for many stars, in this paper we compute the ages of transiting-planet host stars (TPH) in a homogeneous way via isochrones. Knowledge of stellar ages is particularly important in the context of planet-hosting stars (SWP). The age distribution of SWP tells us whether planets are preferentially hosted by young or old stars. This is related to the dynamical stability of the systems and with the mutual influence between planets and hosting star; see e.g. Pätzold et al. (2004), Barker & Ogilvie (2009), Debes & Jackson (2010). Moreover, ages for exoplanet host stars enable a comparison with typical timescales of biological evolution and an assessment of the plausibility of the presence of life (see e.g. Kasting & Catling 2003).

The paper is organised in the following way: Sect. 2 describes the characteristics of our stellar sample and the isochrones. Section 3 presents the central aspects of our algorithm, Sect. 4 shows the results, and Sect. 5 summarizes our work.

2. The data

2.1. Planet-hosting stars catalogues

We analysed the ages of those stars whose planets were discovered through the transit method. In principle, these kinds of

stars should not suffer from biases: (1) the stars that are chosen are not necessarily inactive, unlike in radial velocity surveys, where spectroscopic analysis requires sharp and well-defined lines. However, we caution that it is indeed more difficult to detect transits for stars with a large amplitude of intrinsic variability. (2) These TPH stars are not necessarily slow rotators, unlike in radial velocity surveys. In fact, rotation broadens the lines and reduces their depth, making spectroscopic analysis less precise, however, once a possible transit signal is detected, spectroscopic validation is required to confirm such a planet. Therefore, stars belonging to photometric surveys must also be suitable for spectroscopic analyses if exoplanet validation is expected, so almost the same biases are expected. In fact, in the case of transiting planet hosts, there are other systematic selection effects. Transiting-planet hosts are expected to be preferentially edge-on, even if spin-orbit misalignment occurs in some exoplanetary systems. Gravity darkening or differential rotation (von Zeipel 1924; Maeder 1999) could affect stellar observables. In addition, the hosted planets are very close to their own star.

We selected 61 transiting-planet hosts from SWEET-Cat, a catalogue of stellar parameters for stars with planets[1] (Santos et al. 2013), to obtain our transiting-planet hosts (TPH) catalogue. Among the stars of this catalogue, we further consider only those stars brighter than $V = 12$ and this inevitably introduces a further source of bias. This criterion takes into account that future photometric missions with the aim of characterizing exoplanets, such as CHEOPS (Broeg et al. 2013) or PLATO (Rauer et al. 2014), will investigate bright stars. This led us to the Bright Transiting-Planet Hosts (BTPH) catalogue, which is composed of 43 stars. The metallicity [Fe/H] and the logarithm of the surface gravity $\log g$ are always available from Sweet-Cat. If available, we took V magnitude and $B - V$ colour index from Maxted et al. (2011), otherwise we collected V from SWEET-Cat and $B - V$ from The Site of California and Carnegie Program for Extrasolar Planet Search: Exoplanets Data Explorer[2]. As reported by Maxted et al. (2011), the target stars of surveys that aim to discover exoplanets through transits are typically characterized by optical photometry of poor quality in the range $V = 8.5-13$ mag. For stars brighter than $V \approx 12$, optical photometry is usually available from Tycho catalogue, nevertheless, this catalogue is only complete up to $V \approx 11$ and photometric accuracy rapidly deteriorates for $V \gtrsim 9.5$. The authors give high-quality photoelectric optical photometry for planet-hosting stars (mostly WASP discoveries), so we decided to use these data if available.

We also built a catalogue of 274 planet-hosting stars whose planets were detected through radial velocity method (spectroscopic hosts: SH catalogue) from SWEET-Cat.

2.2. Solar neighbourhood catalogues

We built a catalogue of F-G-K main sequence stars (MS-stars) belonging to the solar neighbourhood (SN catalogue) by taking stellar data from the re-analysis of the Geneva-Copenhagen survey by Casagrande et al. (2011). It is a survey of late-type dwarf stars that are magnitude limited at $V \approx 8.3$; the authors computed the ages for these stars. In particular, we collected the 7044 stars with available ages, belonging to the MS. The MS containing the F-G-K stars has been indentified by selecting a strip going from $T_{\rm eff} \approx 4500$ K to $T_{\rm eff} \approx 7100$ K, within a range of 0.45 dex in $\log L$, whose minimum and maximum values are -1.24 dex and 0.63 dex, respectively. We further removed F type stars, i.e stars with $T_{\rm eff} > 6300$ K, from the SN catalogue. This way we remained with 3713 stars (Reduced Solar Neighbourhood catalogue; RSN) belonging to the same spectral type range of planet-hosting stars. Among useful input parameters to compute stellar ages through our own algorithm, Casagrande et al. (2011) give only metallicity, which is inferred from Strömgren photometry; distance, according to the new reduction of the HIPPARCOS parallaxes (van Leeuwen 2007); and V magnitude for each star. We complemented this information by cross-matching the entire Geneva-Copenhagen survey with the catalogue of cool late-type stars by Valenti & Fischer (2005), which also provides precise spectroscopic measurements of surface gravity $\log g$ and projected rotational velocity $v \sin i$. This led to the Valenti Fischer Solar Neighbourhood catalogue (VF-SN catalogue), which contains 825 stars.

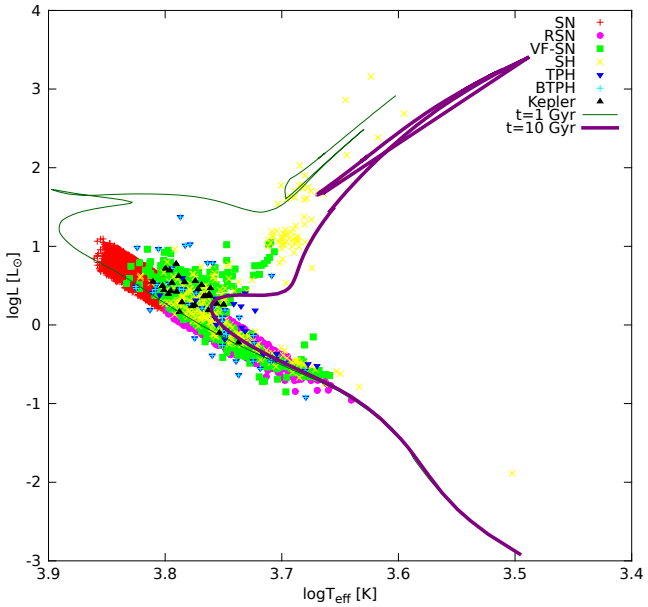

Fig. 1. Stars belonging to our custom-built catalogues are represented on the HRD. Two solar metallicity isochrones, corresponding to 1 Gyr and 10 Gyr, are shown as reference. Since BTPH is a subsample extracted from TPH, all the cyan crosses representng the BTPH stars are superimposed on part of the blue reverse triangles representing the TPH stars.

A brief overview of our custom-built catalogues used in the paper is given in Table 1. In Fig. 1 stars, belonging to our catalogues are represented on the HRD with two solar metallicity isochrones as reference.

2.3. Isochrones

To compute the ages of stars we used isochrones taken from Padova and Trieste Stellar Evolutionary Code (PARSEC, version 1.0)[3] by Bressan et al. (2012). We queried isochrones identified by $\log t$ in the range between 6 and 10.1 (t in years) at steps of 0.05 dex. These isochrones include the pre-MS phase, so the given ages must be considered as starting from the birth of a star and not since the zero age main sequence (ZAMS). Specific details about the solar parameters adopted by the isochrones are already reported by Bonfanti et al. (2015). Here, we recall the relation between metallicity Z and [Fe/H], i.e.

$$Z = 10^{[\rm Fe/H]-1.817} \quad (1)$$

[1] https://www.astro.up.pt/resources/sweet-cat/
[2] http://exoplanets.org/table
[3] http://stev.oapd.inaf.it/cgi-bin/cmd

Table 1. Overview of our custom-built catalogues.

Catalogue	# Stars	log g source	Reference
TPH: Transiting planet hosts	61	spectroscopy	SWEET-Cat
BTPH: Bright transiting planet hosts	43	spectroscopy	SWEET-Cat
SH: Spectroscopic hosts	274	spectroscopy	SWEET-Cat
SN: Solar neighbourhood	7044	not available	Casagrande et al. (2011)
RSN: Reduced solar neighbourhood	3713	not available	Casagrande et al. (2011)
VF-SN: Valenti Fischer solar neighbourhood	825	spectroscopy	Casagrande et al. (2011) + Valenti & Fischer (2005)
Kepler sample[a]	29	asteroseismology	Silva Aguirre et al. (2015)

Notes. [(a)] See Sect. 4.1.

3. Age determination methods

Computing the age of a field star through isochrones requires us to put the star on a suitable plane with its error bars. Traditionally, HRD is chosen, so $T_{\rm eff}$ and L are the reference quantities. Several catalogues in the literature already report $T_{\rm eff}$ or L, but they were obtained by different authors through different processes and/or calibration techniques. For instance, $T_{\rm eff}$ and L are not likely to be consistent with the colour-temperature scale or the bolometric corrections (BCs) adopted by the isochrones. Therefore, we prefer to start from quantities coming from observations in a straightforward way, where possible. Our reference input quantities to compute stellar ages are V magnitude, $B-V$ colour index, [Fe/H] metallicity, spectroscopic log g, and parallactic distance d, which can be substituted by the $\frac{a}{R_\star}$ parameter coming from transit, as better specified in Sect. 3.1.

3.1. Isochrone placement: Preliminary considerations

Starting from observational quantities, $T_{\rm eff}$ can be inferred from colour index (e.g. $B-V$), while L is determined thanks to the magnitude in a given band (say V), its corresponding bolometric correction BC_V and the distance d of the star recovered from parallax π. In the particular case where a star hosts a transiting planet, we are able to compute L, even if d is not available. In fact, the ratio between the orbital period P and the transit duration allows us to recover $a/R_\star$, where a is the planet semi-major axis and $R_\star$ is the stellar radius (see e.g. Winn 2010). Rearranging Kepler III law in the manner shown by Sozzetti et al. (2007), the mean stellar density results to be

$$\rho_\star = \frac{3\pi}{G}\left(\frac{a}{R_\star}\right)^3 \frac{1}{P^2} \tag{2}$$

where G is the universal gravitational constant. Combining the spectroscopic log g with $\rho_\star$, one can solve a system of two equations in the two variables $R_\star$ and $M_\star$. One obtains

$$\begin{cases} \dfrac{R_\star}{R_\odot} = \dfrac{g}{g_\odot}\left(\dfrac{\rho_\star}{\rho_\odot}\right)^{-1} \\ \dfrac{M_\star}{M_\odot} = \left(\dfrac{g}{g_\odot}\right)^3\left(\dfrac{\rho_\star}{\rho_\odot}\right)^{-2}. \end{cases} \tag{3}$$

Finally, the stellar luminosity L is given by

$$\frac{L}{L_\odot} = \left(\frac{R}{R_\odot}\right)^2\left(\frac{T_{\rm eff}}{T_{\rm eff,\odot}}\right)^4. \tag{4}$$

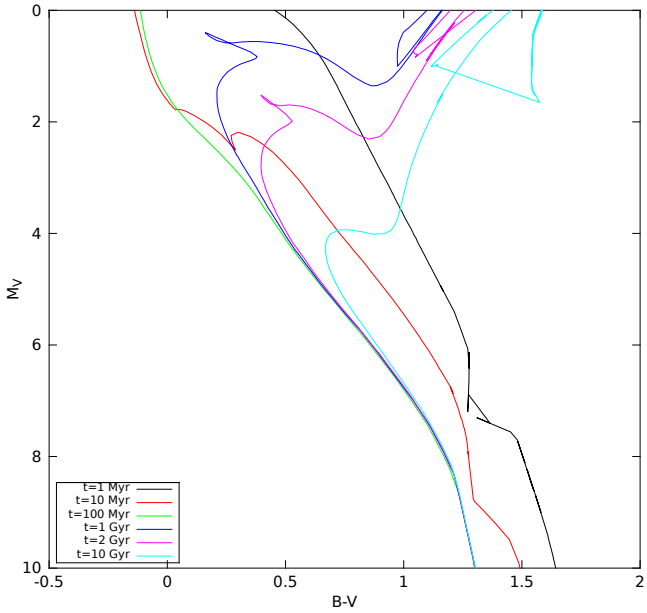

Fig. 2. Isochrones of solar metallicity: pre-MS isochrones are located on the right-hand side of the MS (in this region ages increase from right to left on the diagram) and they intersect older isochrones around the TO. The ages of MS isochrones increase from left to right on the diagram.

In Bonfanti et al. (2015) we have already pointed out that on the right-hand side of the main sequence (in the lower temperature region) or around the turn-off (TO) very old and very young isochrones are close and can even overlap. According to Fig. 2, the 1-Myr- and 10-Myr-isochrones interesect older isochrones in the TO region. The intersection points are representative of a degeneracy between pre-MS and MS isochrones on the CMD. In fact, the photometry alone cannot disentagle young and old ages, and other information is needed.

So far, the only exoplanet candidate orbiting around a pre-MS is PTFO 8-8695b, as reported by van Eyken et al. (2012) and then investigated by Barnes et al. (2013). Thus, we do not expect to find pre-MS stars among our samples of stars with planets. Anyway, our algorithm is built to compute ages of any kind of star and we decided to perform the activity checks that are described in the following. In this way, we do not put any a priori conditions on the evolutionary stage of the planet-hosting stars. Possible pre-MS interlopers in our planet-hosting stars samples would be very low-mass stars with long pre-MS lifetimes. Twenty-two stars out of the 335 SWP have masses lower than 0.8 $M_\odot$. In principle, they could be pre-MS stars and the checks performed by our algorithm may help in recognizing them.

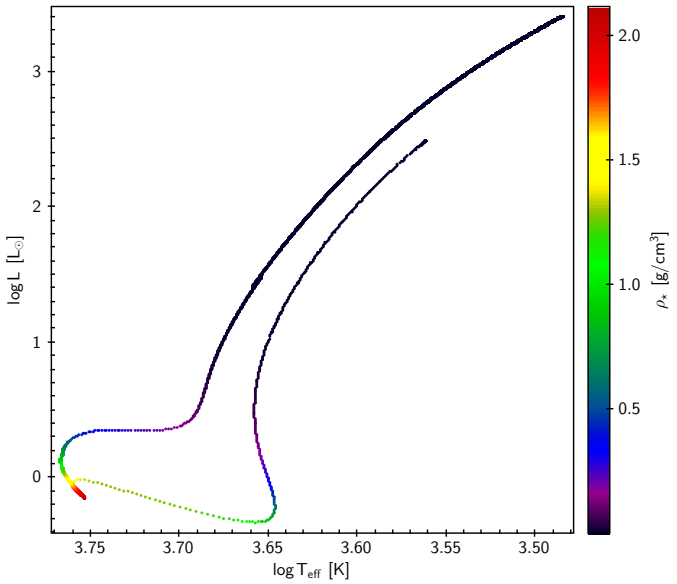

Fig. 3. Evolutionary track of a star with $M = 1 M_\odot$ and $Z = Z_\odot$. Even if the oldest MS isochrones are close to pre-MS isochrones, however, $\rho_\star$ in the MS is sensibly higher with respect to the pre-MS phase. As a consequence, the mean stellar density enables us to discard unlikely age values according to $\rho_\star$.

In the case of late spectral type stars, such as those analysed in this paper, very young stars are chromospherically very active with respect to older stars and typically rotate faster, so we performed activity checks in terms of $\log R'_{HK}$ and $v \sin i$, trying to remove the degeneracy between pre-MS and MS isochrones. We evaluated three age scales through three independent methods to decide on the ensemble of isochrones to be used in the following computation.

1. We considered the age-activity relation by Mamajek & Hillenbrand (2008) and we set a conservative threshold of 0.2 dex corresponding to the typical difference between the highest and lowest peaks in activity and the average level for a solar-type star. Inserting $\log R'_{HK}$ in the relation, we evaluated the corresponding age: τ_{HK} represents this age if it was younger than 500 Myr, otherwise $\tau_{HK} = 500$ Myr.
2. Meibom et al. (2015) proved that the gyrochronological relation by Barnes (2010) holds up to 2.5 Gyr, so we applied this relation employing $\frac{4}{\pi} v \sin i$ as the expected stellar rotational velocity to obtain the gyro age τ_v. We set $\tau_v = 2.5$ Gyr, if the resulting gyro age was older than 2.5 Gyr.
3. There is other information that may suggest whether a star located under the TO on the right-hand side of the MS is very young or very old, and this is $\rho_\star$. Figure 3 shows the evolutionary track of a 1 $M_\odot$ star with solar metallicity. Starting from the birth of a star, $\rho_\star$ increases in approaching the MS. After the TO, $\rho_\star$ clearly decreases so that post-MS stars have a mean stellar density similar to that of pre-MS stars. So, for $M_V > 5$, corresponding to the luminosity of the TO of the oldest isochrone in the CMD, pre-MS isochrones differ from older isochrones in terms of $\rho_\star$. Among pre-MS ages, τ_ρ is the threshold age value such that for $t < \tau_\rho$ isochrones report mean stellar density $\rho < \rho_\star$.

The maximum value among τ_{HK}, τ_v and τ_ρ represents the age up to which all the younger isochrones are discarded before the computation of stellar age.

3.2. Isochrone placement: Implementation

The isochrone placement technique enables the determination of the ages of field stars, as well as all the other stellar parameters, such as $T_{\rm eff}$, L, $\log g$, $M_\star$, $R_\star$, according to stellar evolutionary models. This technique was already described in Bonfanti et al. (2015), but several improvements have been made, such as the new kind of activity checks described above and the possibility of computing the age without any input distance d, if we have stellar density measurements. We also solved some problems linked to numerical stability convergence for which the previous algorithm sometimes gave fictitious young ages. In fact, in the previous version of the algorithm some input data were loaded in single precision, instead of double precision. Sometimes, it could happen that single precision were not sufficient to perform the correct computation of stellar parameters. Moreover, we make this new version more flexible, since it also enables to use input asteroseismic global parameters or only spectroscopic parameters if photometry is not available. Here, we briefly summarize the key aspects.

To make as few assumptions as possible and to start from input data directly obtained from observations, our algorithm requires

- visual magnitude V;
- colour index $B - V$;
- metallicity [Fe/H];
- spectroscopic $\log g$;

and the distance d or $a/R_\star$. If d is available, it is possible to infer $T_{\rm eff}$ from $B - V$ and L from the absolute magnitude M_V via interpolation in the isochrone grid. Then $R_\star$ is known thanks to Stefan-Boltzmann law (Eq. (4)) and finally $M_\star$ can be computed by combining $R_\star$ with $\log g$. If, instead, d is not available, which can occur for some TPH, first we compute $\rho_\star$ through (2) and then we recover $M_\star$ and $R_\star$ via relations (3). After that, we obtain the correspondence between $B - V$ and $T_{\rm eff}$ through interpolation in the isochrone grid. Finally, we compute L from $T_{\rm eff}$ with (4). Once all the input parameters are available, it is possible to derive stellar properties according to Padova theoretical models by properly weighting each isochrone in the manner already described in Bonfanti et al. (2015). With the new version of the algorithm, we improved the weighting scheme to take the evolutionary speed of a star into account. In fact, the probability that a star is a given age does not only depend on the simple distance between the star and the given isochrone in the HRD, but it is also influenced by the time spent by a star in a given evolutionary stage. For instance, pre-MS evolution is quicker than the MS one. This means that a star rapidly changes its properties during the first tenths of Myr of its life, instead, it remains in the MS for Gyrs with parameters variations detectable on longer timescales. As a consequence, given a star on the HRD, located at the same distance with respect to a pre-MS and a MS isochrone, the probability of dealing with a MS star is higher. To quantify this aspect, we considered the theoretical stellar evolutionary track characterized by the same input metallicity and mass of the star, and we evaluated its evolutionary speed by

$$v_{\rm evo} = \sqrt{\left(\frac{\log L_2 - \log L_1}{t_2 - t_1}\right)^2 + \left(\frac{\log T_{\rm eff,2} - \log T_{\rm eff,1}}{t_2 - t_1}\right)^2} \qquad (5)$$

where $(\log T_{\rm eff,1}, \log L_1)$ is the point on the track, that is nearer to the star, while $(\log T_{\rm eff,2}, \log L_2)$ is the point that occurs later in time on the track, and t_1 and t_2 are the epochs reported by the

track. The greater $v_{\rm evo}$, the less is the probability to find a star in such an evolutionary stage. We normalized $v_{\rm evo}$, with respect to a reference speed value $v_{\rm ref}$ for a given track, that is the lowest speed registered on the entire track. In this way, the evolutionary speed can be easily interpreted as a multiple of a reference speed with which a star goes along its track and the contribution to be added to the weight is unitless, like the others. So the weight p_i to be attributed to the ith isochrone results to be

$$p_i = \left[\left(\frac{\log L - \log L_i}{\Delta\log L}\right)^2 + \left(\frac{\log T_{\rm eff} - \log T_{{\rm eff},i}}{\Delta\log T_{\rm eff}}\right)^2 + \left(\frac{M_\star - M_{\star,i}}{\Delta M_\star}\right)^2 + \left(\frac{\log g - \log g_i}{\Delta\log g}\right)^2 + \log^2\left(\frac{v_{\rm ref}}{v_{\rm evo}}\right)\right]^{-1} \cdot \quad (6)$$

Sometimes photometry is not available and only spectroscopic analyses have been carried out. We caution that the given spectroscopic input temperature has been inevitably subjected to a calibration process, which can bring biases. Anyway, to compute ages in such cases we can use spectroscopic [Fe/H], $T_{\rm eff}$ and $\log g$. In this case, the algorithm works in the $\log g$–$\log T_{\rm eff}$ plane following the same prescriptions as in the HRD. This time the weight is simply given by

$$p_i = \left[\left(\frac{\log g - \log g_i}{\Delta\log g}\right)^2 + \left(\frac{\log T_{\rm eff} - \log T_{{\rm eff},i}}{\Delta\log T_{\rm eff}}\right)^2 + \log^2\left(\frac{v_{\rm ref}}{v_{\rm evo}}\right)\right]^{-1} \quad (7)$$

where the evolutionary speed of the star $v_{\rm evo}$ and its reference value $v_{\rm ref}$ are evaluated in the $\log g$–$\log T_{\rm eff}$ plane instead of the HRD.

If global asteroseismological indexes, i.e. $\Delta\nu$ and $\nu_{\rm max}$, are available, $\log g$ and $\rho_\star$ may also be computed by inverting the following scaling relations:

$$\Delta\nu = \sqrt{\frac{M_\star}{M_\odot}\left(\frac{R_\star}{R_\odot}\right)^{-3}}\,\Delta\nu_\odot \quad (8)$$

$$\nu_{\rm max} = \frac{g}{g_\odot}\left(\frac{T_{\rm eff}}{T_{{\rm eff},\odot}}\right)^{-\frac{1}{2}}\nu_{{\rm max},\odot} \quad (9)$$

$\Delta\nu_\odot = 135.1\,\mu$Hz and $\nu_{{\rm max},\odot} = 3090\,\mu$Hz as reported by Chaplin et al. (2014). Knowledge of both $\log g$ and $\rho_\star$ enables us to compute $M_\star$ and $R_\star$. Given that $T_{\rm eff}$ is available, L may also be recovered using (4). Even if an accurate asteroseismological analysis based on the study of individual frequency enables precise determination of the stellar evolutionary stage, however, combining information from global asteroseismic parameters and from spectroscopy gives a complete set of input data useful for our isochrone placement. Once the star is located on the HRD, it is then possible to compute its age and its parameters according to Padova evolutionary models. Our algorithm takes element diffusion into account.

If known, stellar multiplicity has been pointed out through a flag at the column *Bin* of Table A.1. In these cases, the literature already reports data referred to the specific star we analysed. We caution that if some unresolved binaries were present in our samples, such stars would appear more luminous than they are. If located in the MS region, they would erroneously be judged as older.

Another critical point deals with reddening. In the case of SWP, we do not deeply check whether the different sources give photometry de-reddened or not because neither *SWEET-Cat* nor the *Exoplanets Data Explorer* report any reddening information. We explicitely account for reddening in the case of those TPH listed in Maxted et al. (2011), who report the colour excess $E(B-V)$. Anyway, by a posteriori catalogue cross-matching, we were able to recover $E(B-V)$ index for 154 stars out of the 335 SWP, and we found that more than 80% of them has $E(B-V) = 0$. Similarly, ∼90% of the stars belonging to the VF-SN catalogue have $E(B-V) = 0$. Considering also that the analysed stars are essentially inside the Local Bubble, whose extension varies between ∼80 and 200 pc from the Sun (Sfeir et al. 1999), we expect that the effect of reddening does not significantly impact our resulting statistics.

4. Results

4.1. Test of the algorithm

Silva Aguirre et al. (2015) analysed a sample of *Kepler* exoplanet host stars (*Kepler* sample from here on). They performed a complete asteroseismological analysis of the individual oscillation frequencies, recovered thanks to the high signal-to-noise ratio of their observations. Among other fundamental properties, they derived the ages of their sample of stars, claiming a median error of 14%. As a result of high reliability attributed to a complete asteroseismological analysis, comparing the results given by our isochrone placement with those reported by Silva Aguirre et al. (2015) represents a good validation test for our algorithm. The authors observe that the majority of these stars are older than the Sun because of selection effects. In particular, stellar pulsations characterized by high signal-to-noise ratio are preferentially detected in F-type stars (ages ∼2–3 Gyr) and in old G-type stars (ages ∼6 Gyr). Thus, aim of this section is to test the accuracy of our algorithm, without comparing the evolutionary stage of the *Kepler* sample with other stars.

We analysed 29 over 33 stars of the *Kepler* sample, for which both $\Delta\nu$ and $\nu_{\rm max}$ were available. We have just considered the global asteroseismic parameters, deriving input $\log g$ and $\rho_\star$ by inverting (8) and (9). Spectroscopic [Fe/H] and $T_{\rm eff}$ were reported by Silva Aguirre et al. (2015). If available, $v \sin i$ was employed to perform checks as described in point 2 in Sect. 3.1.

Our age determination is in good agreement with the analysis of Silva Aguirre et al. (2015), as shown in Fig. 4. The linear correlation coefficient $r = 0.95$ and the reduced $\chi^2/26 = 1.5$ confirm that a linear least-squares regression well describe the data scatter and is consistent with the extension of our error bars. The least-squares line represented in green (thicker line) shows that our method slightly overestimate the age in the domain of the oldest stars.

4.2. The ages of the exoplanet hosts

The BTPH catalogue is a subset of the TPH catalogue. In Fig. 5, we superimposed the age distribution of the 43 stars belonging to the BTPH catalogue (grey bars) to the age distribution of the all TPH (blue bars). The medians of the distributions are ∼4.2 Gyr and ∼5 Gyr for the BTPH and for the TPH, respectively. One of the three stars younger than 1 Gyr, namely WASP-18 ($t = 0.9 \pm 0.2$ Gyr), appears too blue for its metallicity, so we investigated the input parameters of this star. Southworth et al. (2009) analysed the properties of WASP-18, adopting $V = 9.30$ and $B-V = 0.44$, instead of $V = 9.273$ and $B-V = 0.484$, which are the values we used. In addition they started from [Fe/H] = 0, as reported by Hellier et al. (2009), which sensibly differs from [Fe/H] = 0.19, which we took from SWEET-Cat. With the input

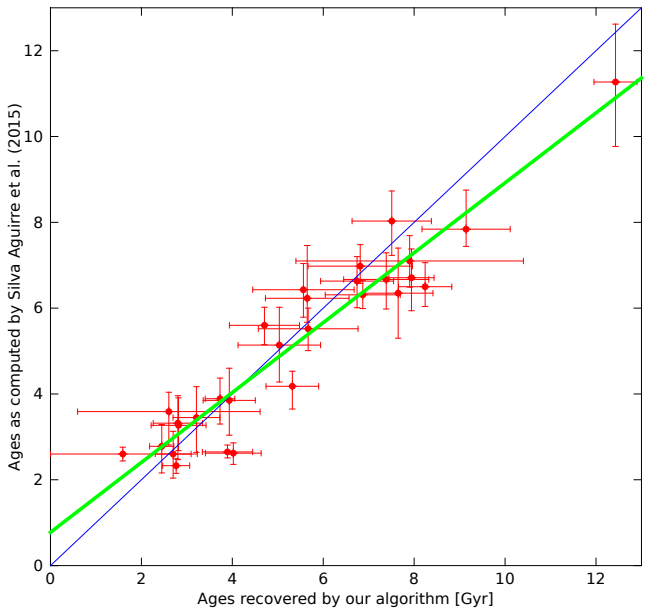

Fig. 4. Ages of the *Kepler* sample. The least-squares line that regress the data is represented with a thick green line, while the thin blue line is the bisector representing the exact correspondence between the data.

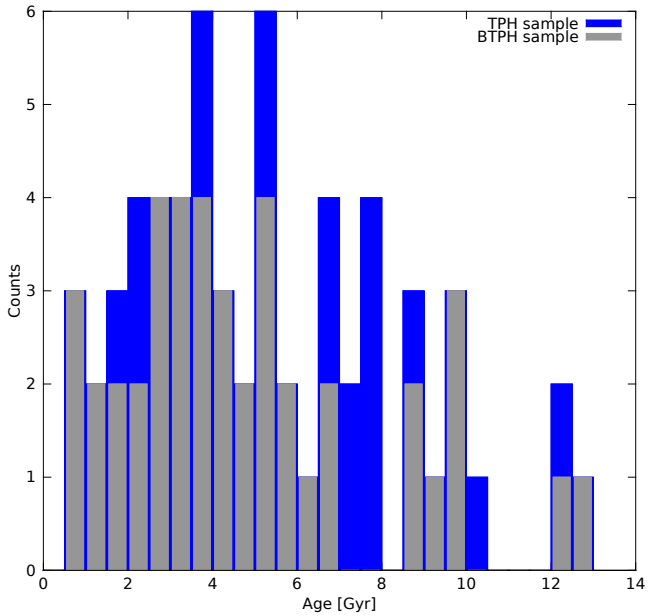

Fig. 5. Grey bars represent age distribution of the 43 stars belonging to the BTPH catalogue. The superset given by TPH catalogue is represented in the background through blue bars.

parameters used by Southworth et al. (2009), WASP-18 is again located on the bluer side out of the MS, and our isochrone placement gives $t = 0.2^{+0.3}_{-0.2}$ Gyr. Southworth et al. (2009) considered different sets of evolutionary models and they concluded that WASP-18 is age between 0 and 2 Gyr. This is consistent with both of our determinations, but since the different sets of input parameters do not fully agree with Padova theoretical models, we caution that the age estimation is not necessarily reliable. Further photometric investigations or a re-determination of its metallicity are required to correct the inconsistency between the position of the star on the HRD and the theoretical isochrones.

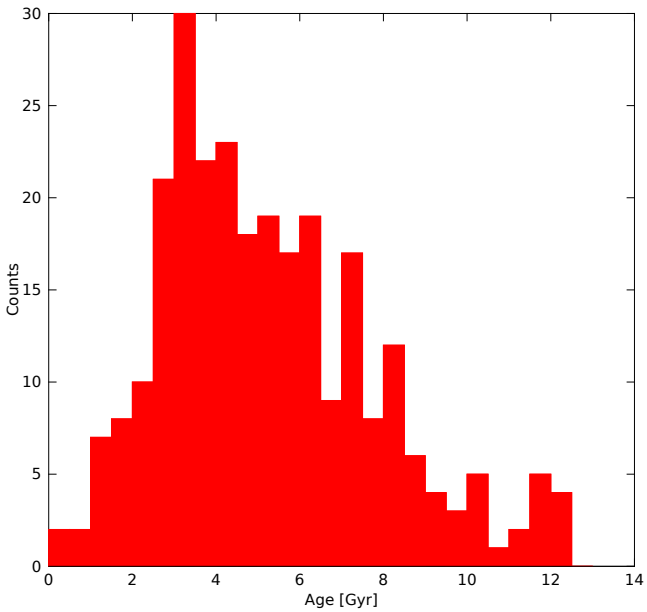

Fig. 6. Age distribution of the 274 stars belonging to the SH catalogue. The median of the distribution is ~4.8 Gyr, which is very close to the age of the Sun.

As a term of comparison, we computed the ages of stars taken from SH catalogue. The consequent age distribution is represented in Fig. 6. This age distribution peaks in the [3, 3.5) Gyr bin and its median is ~4.8 Gyr, which is very close to the solar age value. The age distributions in Figs. 5 and 6 are consistent. Differences may arise because of the paucity of the TPH, but, in any case, no significant bias emerges in the comparison between the samples. Actually, we performed a Kolmogorov-Smirnov test (KS test) to investigate whether TPH and BTPH come from the same distribution, which characterizes the larger SH sample. The high p-values (0.5 for the TPH-SH comparison and 0.3 for the BTPH-SH comparison) suggest that we should not reject the null hypothesis based on which the samples come from the same distribution. This emphasizes that even if photometric and spectroscopic targets could be chosen according to different criteria, the confirmation of a candidate exoplanet requires the application of both the transit and radial velocity method. Therefore, similar biases are expected in the two different samples.

All the parameters of the planet-hosting stars derived according to Padova isochrones are listed in Table A.1.

4.3. Age comparison with the stars of the solar neighbourhood

Our second step is to investigate whether exoplanet hosts are peculiar with respect to field stars not harbouring planets. The exoplanet hosts known so far are late spectral type stars located in the solar neighbourhood: ~90% of the planet-hosting stars we analysed are closer than 200 pc. The stars contained in the SN catalogue represent an interesting comparison test because they represent a numerous sample of late spectral type MS-stars occupying almost the same volume as the exoplanet hosts. The age values reported by Casagrande et al. (2011, C11 from here on) are computed following their own method, so we checked whether their results were consistent following the VF-SN subsample, which contains all the input parameters needed by our algorithm. We managed to obtain the age for 818 stars. We recall

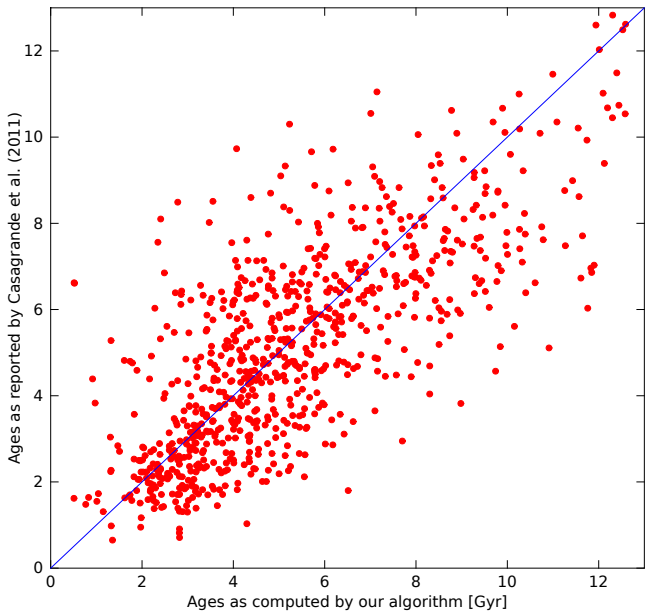

Fig. 7. Age comparison between Casagrande estimation and ours (818 stars). The dispersion between the two measurements can be quantified through the linear correlation coefficient, that is ~0.75.

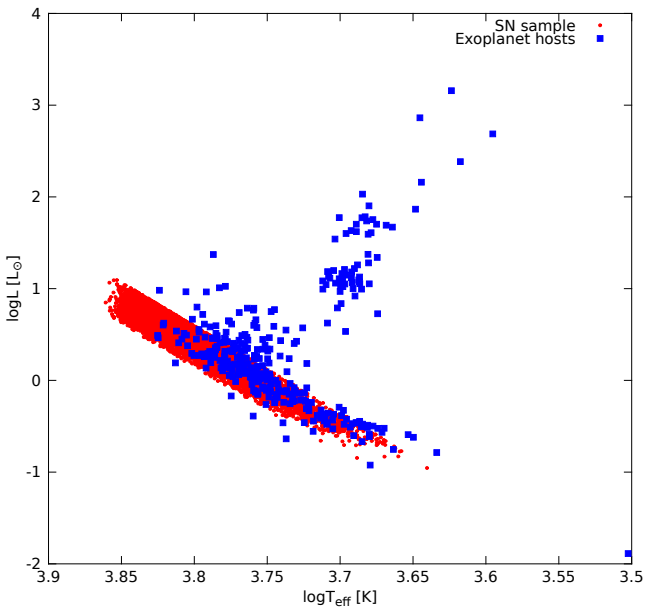

Fig. 8. SN sample on the HRD (red dots). The very straight boundaries of the SN sample is simply a consequence of our identification of the MS through a strip as described in Sect. 2.2. All the planet-hosting stars we analysed are superimposed (blue squares).

that the cut in spectral type is imposed by both C11 and Valenti & Fischer (2005) limits, and includes basically F, G and K stars. The plot of the expectation age reported by C11 versus our age values is shown in Fig. 7. The scatter of points around the bisector is expected given the high age uncertainties, and, in any case, good statistical agreement characterizes the two determinations. The median age for C11 values is ~4.9 Gyr, which is very similar to our median age (~4.8 Gyr) for the common sample. This agreement between the two age determinations suggests that any comparison between C11 ages and ours is consistent. In addition, considering the median age value coming from the VF-SN sample, it is not surprising that the age is similar to the ages found for the samples of stars with planets analysed above. In fact, we obtained the VF-SN catalogue by cross-matching the SN sample with the catalogue of stars reported by Valenti & Fischer (2005). The authors performed high-precision spectroscopy on stars taken from Keck, Lick and AAT planet search programme, thus, their stars present the typical selection effects characterizing stars with planets. Actually the median value we obtained for the VF-SN sample is the same as the SH value.

As C11 age values suggest, the age distribution of all the 7044 stars belonging to the SN catalogue peaks in the [1.5, 2) Gyr bin with a median age value of ~2.6 Gyr. This raw analysis may suggest that field stars are globally younger than planet-hosting stars. Instead, this comparison hides a bias, in fact, the SN catalogue contains a huge number of hot F-type stars with respect to planet-hosting stars, as shown in Fig. 8 (stars with $\log T_{\rm eff} \gtrsim 3.8$). The earlier the spectral type, the faster the evolution of a star, thus, F-type stars are expected to be statistically younger than later spectral type stars.

Analysing Fig. 8, all the stars with $T_{\rm eff} > 6300$ have been removed from the SN catalogue, remaining with 3713 stars (RSN catalogue). In this way, the comparison between the solar neighbourhood stars and the stars with planets is homogeneous in spectral type. The result is given by the age distributions in Fig. 9. They are almost consistent (KS p-value is 0.2): SN age distribution is less peaked, but they both have 4.8 Gyr as median value.

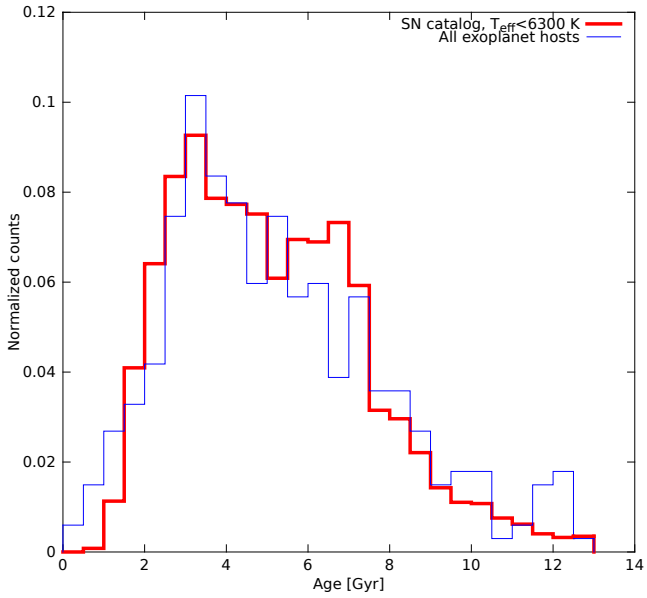

Fig. 9. Age distribution of the MS stars colder than 6300 K belonging to the RSN catalogue (red stairs, 3713 stars) compared with the age distribution of all the planet-hosting stars we analysed (blue stairs, 335 stars).

Two considerations should be added.

1. The median age value of the stars with planets is very similar to the solar age value, but very different (~1 Gyr) from the histogram peak because of the extended tail towards old ages. According to their metallicities, there is no evidence that planet-hosting stars with $t \gtrsim 9$ Gyr have population II properties. If we exclude this contamination, we may argue whether such a skew distribution may be due to a real distribution reflecting a prolonged star formation history (Rocha-Pinto et al. 2000) or to an asymmetric propagation of errors.
2. Assuming a solar age of ~4.6 Gyr (Chaussidon 2007), an age of t = 4.6–4.8 Gyr appears older than that currently assumed

for most of the thin disc population, where planet-hosting stars and the RSN sample are located. In fact, as summarized by Allende Prieto (2010), Reddy et al. (2006) say that thin disc stars span a range between 1 and 9 Gyr, with the majority of them younger than 5 Gyr. Holmberg et al. (2009) and Haywood (2008) set an older upper limit for the thin disc ages, however they both agree that most of these stars are younger than 4–5 Gyr. Rocha-Pinto et al. (2000), using a different approach based on the stellar activity as age indicator, found three different peaks in the local star formation history, with the highest at very young ages below 1 Gyr. We caution that we limited our sample primarily to G-type stars. The other point is that we are sampling a very limited inter-arms volume (essentially <200 pc), as most of the recent studies based on single star age measurements. The literature does not present detailed studies of the ages of single disc stars far away from the solar neighbourhood. Thus, this lack of information does not allow us to perform a complete comparison between the evolutionary properties of our samples and those of the entire galactic disc. The extension of the stellar analysis to a distance larger than 200 pc would include younger active star-forming regions, such as the Orion Nebula or Taurus-Auriga complex. As a consequence, in deeper surveys we expect to include significantly younger stars.

5. Conclusions

We analysed a sample of 61 transiting-planet hosts to compute their ages and their peculiar parameters according to Padova isochrones. A priori, one could say that our particular sample is expected not to be affected by some typical biases that characterize those planet-hosting stars coming from radial velocity surveys. Spectroscopic targets are often deliberately chosen to be slow rotators and typically inactive. Instead, very high-precision photometry only requires bright stars in the solar neighbourhood for an adequate signal-to-noise ratio. Actually, once a possible transiting planet has been detected, the confirmation process involves spectroscopic analysis. Therefore, similar biases are expected in both spectroscopic and photometric surveys.

We found that the median age of our TPH sample is ∼5 Gyr. The subsample of TPH brighter than $V = 12$ yields a median age of ∼4.2 Gyr. This slightly lower value is expected since brighter stars are on average younger. In order to comment the age distribution of TPH, we also considered 274 planet-hosting stars, whose planets have been detected though radial velocity method. Their age distribution peaks in the [3, 3.5) Gyr bin and it is synthesized by a median value of ∼4.8 Gyr. These three samples of stars are consistent from an evolutionary point of view. Slight differences are due to the paucity of stars belonging to the TPH catalogue and, in fact, a KS test does not suggest that TPH and SH come from a different distribution. Thus, spectroscopic and photometric targets are characterized by almost the same selection effects, and these biases bring the median of their age distribution around the solar age value.

In the second part we checked whether planet-hosting stars have peculiar ages with respect to field stars without planets of the solar neighbourhood. In case of a homogeneous comparison in terms of spectral type, solar neighborhood stars belonging to the RSN catalog have an age distribution very similar to that deriving from the all exoplanet hosts considered in this paper and the median age is ∼4.8 in both cases. With its age of 4.567 Gyr (as reported by Chaussidon 2007), the Sun appears not to be a peculiar star, if compared with both the planet-hosting stars and the SN stars, whose spectral types span essentially from late-F to early K. However, it looks that we are sampling a limited inter-arms region, possibly older than the average thin disc population.

Acknowledgements. We thank the anonymous referee for the interesting and fruitful comments that improved our paper. A.B. and S.O. acknowledge "contratto ASI-INAF n.2015-019-R0 del 29 luglio 2015" and support from INAF through the "Progetti Premiali" funding scheme of the Italian Ministry of Education, University, and Research. S.O. acknowledge financial support from University of Padova, as well. V.N. acknowledges support from INAF-OAPd through the grant "Studio preparatorio per le osservazioni della missione ESA/CHEOPS" (#42/2013). This research has made use of the Exoplanet Orbit Database and the Exoplanet Data Explorer at exoplanets.org. Moreover it has made use of SWEET-Cat: a catalog of stellar parameters for stars with planets at astro.up.pt (Centro de Astrofisica da Universidade do Porto).

References

Allende Prieto, C. 2010, in IAU Symp. 265, eds. K. Cunha, M. Spite, & B. Barbuy, 304
Barker, A. J. & Ogilvie, G. I. 2009, MNRAS, 395, 2268
Barnes, S. A. 2010, ApJ, 722, 222
Barnes, S. A. & Kim, Y.-C. 2010, ApJ, 721, 675
Barnes, J. W., van Eyken, J. C., Jackson, B. K., Ciardi, D. R., & Fortney, J. J. 2013, ApJ, 774, 53
Bonfanti, A., Ortolani, S., Piotto, G., & Nascimbeni, V. 2015, A&A, 575, A18
Bressan, A., Marigo, P., Girardi, L., et al. 2012, MNRAS, 427, 127
Broeg, C., Fortier, A., Ehrenreich, D., et al. 2013, in EPJ Web Conf., 47, 3005
Casagrande, L., Schönrich, R., Asplund, M., et al. 2011, A&A, 530, A138
Chaplin, W. J., Basu, S., Huber, D., et al. 2014, ApJS, 210, 1
Chaussidon, M. 2007, Formation of the Solar system: a chronology based on meteorites, eds. M. Gargaud, H. Martin, & P. Claeys (Berlin: Springer-Verlag), 45
Debes, J. H. & Jackson, B. 2010, ApJ, 723, 1703
Handler, G. 2013, Asteroseismology (Oswalt, T. D. and Barstow, M. A.), 207
Haywood, M. 2008, MNRAS, 388, 1175
Hellier, C., Anderson, D. R., Collier Cameron, A., et al. 2009, Nature, 460, 1098
Holmberg, J., Nordström, B., & Andersen, J. 2009, A&A, 501, 941
Kasting, J. F. & Catling, D. 2003, ARA&A, 41, 429
Kjeldsen, H. & Bedding, T. R. 1995, A&A, 293, 87
Maeder, A. 1999, A&A, 347, 185
Mamajek, E. E. & Hillenbrand, L. A. 2008, ApJ, 687, 1264
Maxted, P. F. L., Koen, C., & Smalley, B. 2011, MNRAS, 418, 1039
Meibom, S., Barnes, S. A., Platais, I., et al. 2015, Nature, 517, 589
Pätzold, M., Carone, L., & Rauer, H. 2004, A&A, 427, 1075
Rauer, H., Catala, C., Aerts, C., et al. 2014, Exper. Astron., 38, 249
Reddy, B. E., Lambert, D. L., & Allende Prieto, C. 2006, MNRAS, 367, 1329
Rocha-Pinto, H. J., Scalo, J., Maciel, W. J., & Flynn, C. 2000, A&A, 358, 869
Santos, N. C., Sousa, S. G., Mortier, A., et al. 2013, A&A, 556, A150
Sfeir, D. M., Lallement, R., Crifo, F., & Welsh, B. Y. 1999, A&A, 346, 785
Silva Aguirre, V., Davies, G. R., Basu, S., et al. 2015, MNRAS, 452, 2127
Soderblom, D. R. 2010, ARA&A, 48, 581
Southworth, J., Hinse, T. C., Dominik, M., et al. 2009, ApJ, 707, 167
Sozzetti, A., Torres, G., Charbonneau, D., et al. 2007, ApJ, 664, 1190
Valenti, J. A. & Fischer, D. A. 2005, ApJS, 159, 141
van Eyken, J. C., Ciardi, D. R., von Braun, K., et al. 2012, ApJ, 755, 42
van Leeuwen, F. 2007, A&A, 474, 653
von Zeipel, H. 1924, MNRAS, 84, 665
Winn, J. N. 2010, ArXiv e-prints [arXiv:1001.2010]

Appendix A: Additional table

Table A.1. Planet-hosting stars parameters determined through Padova isochrones.

Star	t (Gyr)	Δt (Gyr)	$T_{\rm eff}$ (K)	$\Delta T_{\rm eff}$ (K)	L ($L_\odot$)	ΔL ($L_\odot$)	M ($M_\odot$)	ΔM ($M_\odot$)	$\log g$ (cm/s^2)	$\Delta\log g$ (cm/s^2)	R ($R_\odot$)	ΔR ($R_\odot$)	Bin	Tr
11 Com	3.0	0.3	4741	12	109	1	1.37	0.04	2.19	0.02	15.5	0.2	1	0
11 UMi	4.1	1.0	4140	28	243	6	1.4	0.1	1.6	0.04	30.4	0.8	0	0
14 And	5.6	3.0	4775	49	56	1	1.2	0.2	2.4	0.1	11.0	0.3	0	0
14 Her	4.6	1.5	5313	18	0.61	0.01	0.97	0.01	4.48	0.02	0.93	0.01	0	0
16 Cyg B	5.2	1.0	5837	32	1.26	0.01	1.04	0.02	4.37	0.02	1.1	0.02	1	0
18 Del	1.0	0.1	5037	57	35	1	2.1	0.1	2.98	0.04	7.8	0.3	0	0
24 Sex	2.9	0.2	4917	10	16.4	0.1	1.49	0.02	3.11	0.01	5.6	0.04	0	0
30 Ari B	0.4	0.4	6313	24	1.98	0.03	1.25	0.02	4.38	0.01	1.18	0.02	1	0
42 Dra	6.5	1.7	4414	40	145	3	1.1	0.1	1.8	0.1	20.6	0.6	0	0
51 Peg	3.8	1.1	5857	39	1.34	0.03	1.09	0.02	4.37	0.02	1.13	0.03	0	0
55 Cnc	5.1	2.7	5310	32	0.59	0.01	0.95	0.02	4.49	0.03	0.91	0.02	1	1
6 Lyn	3.1	0.4	4973	28	14.8	0.1	1.4	0.1	3.15	0.03	5.2	0.1	0	0
61 Vir	5.2	2.1	5651	36	0.81	0.01	0.96	0.02	4.46	0.03	0.94	0.02	0	0
7 CMa	4.9	1.0	4782	39	11.3	0.2	1.3	0.1	3.17	0.04	4.9	0.1	0	0
70 Vir	8.1	0.4	5560	31	3.0	0.1	1.07	0.01	3.92	0.02	1.9	0.1	0	0
75 Cet	3.3	0.7	4742	14	53.7	0.3	1.4	0.1	2.52	0.03	10.9	0.1	0	0
81 Cet	3.2	0.5	4799	24	59.8	0.4	1.4	0.1	2.49	0.03	11.2	0.2	0	0
91 Aqr	8.1	2.8	4656	26	51	1	1.1	0.2	2.4	0.1	11.0	0.2	0	0
BD +14 4559	6.9	4.2	4948	25	0.32	0.01	0.82	0.02	4.57	0.03	0.78	0.02	0	0
BD +20 2457	10.5	1.7	4504	5	172	12	0.89	0.05	1.71	0.01	21.6	0.8	0	0
CoRoT-18	7.5	4.5	5444	38	0.58	0.04	0.87	0.03	4.5	0.05	0.86	0.04	0	1
CoRoT-19	5.1	0.8	6133	58	3.0	0.3	1.2	0.1	4.12	0.01	1.5	0.1	0	1
CoRoT-7	4.5	4.3	5357	22	0.52	0.05	0.89	0.03	4.54	0.05	0.84	0.05	0	1
HAT-P-11	5.2	3.1	4785	12	0.262	0.004	0.8	0.01	4.59	0.02	0.75	0.01	0	1
HAT-P-13	5.6	0.9	5733	42	2.7	0.2	1.2	0.1	4.071	0.005	1.7	0.1	0	1
HAT-P-14	1.1	0.8	6694	73	4.3	0.3	1.42	0.04	4.21	0.03	1.54	0.08	0	1
HAT-P-17	8.9	2.9	5338	30	0.57	0.01	0.87	0.02	4.48	0.03	0.88	0.02	0	1
HAT-P-22	12.3	0.6	5338	14	0.75	0.01	0.9	0.01	4.37	0.01	1.02	0.01	0	1
HAT-P-24	2.2	1.2	6448	55	2.4	0.2	1.17	0.03	4.30	0.02	1.26	0.06	0	1
HAT-P-26	3.6	0.3	5387	6	0.53	0.01	0.9	0.002	4.541	0.004	0.84	0.01	0	1
HAT-P-27	7.9	2.1	5204	28	0.52	0.01	0.9	0.02	4.49	0.02	0.89	0.01	0	1
HAT-P-36	10.0	0.7	5422	23	0.83	0.01	0.94	0.01	4.37	0.01	1.04	0.02	0	1
HAT-P-4	5.4	0.9	5809	45	2.2	0.1	1.19	0.05	4.169	0.003	1.5	0.1	0	1
HAT-P-7	0.8	0.7	6707	53	5.9	0.7	1.57	0.04	4.12	0.06	1.8	0.1	0	1
HAT-P-9	1.8	0.4	6386	38	2.60	0.04	1.27	0.01	4.29	0.01	1.32	0.03	0	1
HATS-1	7.5	1.1	5705	32	0.95	0.01	0.94	0.01	4.4	0.01	1.00	0.02	0	1
HD 100655	9.4	2.1	4675	4	47	2	1.0	0.1	2.39	0.02	10.4	0.2	0	0
HD 100777	5.9	1.8	5579	37	0.92	0.02	1.00	0.02	4.41	0.03	1.03	0.03	0	0
HD 10180	4.5	1.1	5939	43	1.49	0.03	1.08	0.02	4.34	0.03	1.16	0.03	0	0
HD 101930	5.7	4.3	5144	27	0.42	0.02	0.87	0.03	4.54	0.04	0.82	0.02	1	0
HD 102117	6.1	1.2	5727	47	1.4	0.04	1.07	0.02	4.3	0.03	1.21	0.04	0	0
HD 102195	5.9	3.5	5283	29	0.49	0.01	0.88	0.03	4.53	0.03	0.84	0.02	0	0
HD 102272	11.6	1.2	4794	18	21.5	0.2	0.92	0.03	2.74	0.02	6.7	0.1	0	0
HD 102329	4.1	0.8	4786	39	19.0	0.3	1.4	0.1	2.96	0.04	6.4	0.2	0	0
HD 102365	10.8	2.0	5687	39	0.81	0.01	0.84	0.02	4.42	0.03	0.93	0.02	0	0
HD 102956	2.9	0.2	4892	14	11.9	0.1	1.54	0.02	3.25	0.01	4.8	0.1	0	0
HD 103197	3.4	2.0	5237	18	0.48	0.01	0.91	0.02	4.54	0.02	0.84	0.01	0	0
HD 103774	2.0	0.1	6391	27	3.7	0.1	1.38	0.01	4.183	0.002	1.56	0.03	0	0
HD 104067	9.0	3.4	4961	12	0.31	0.01	0.78	0.01	4.57	0.02	0.75	0.02	0	0
HD 104985	4.9	1.2	4730	41	51	1	1.2	0.1	2.5	0.1	10.6	0.3	0	0
HD 106252	6.4	1.4	5881	47	1.37	0.04	1.02	0.02	4.33	0.03	1.13	0.03	0	0
HD 106270	3.8	0.2	5570	123	5.9	0.3	1.37	0.03	3.74	0.05	2.6	0.2	0	0
HD 10647	1.8	0.9	6159	39	1.56	0.02	1.12	0.02	4.4	0.02	1.1	0.02	0	0
HD 10697	7.5	0.4	5674	93	2.8	0.04	1.12	0.01	4.00	0.03	1.7	0.1	0	0
HD 107148	4.0	1.0	5789	36	1.34	0.05	1.1	0.01	4.35	0.03	1.15	0.03	0	0
HD 108147	1.3	0.5	6211	21	1.88	0.02	1.21	0.01	4.37	0.01	1.19	0.01	0	0
HD 108863	3.3	0.5	4876	29	16.5	0.3	1.4	0.1	3.08	0.03	5.7	0.1	0	0
HD 108874	6.3	0.7	5647	19	1.06	0.01	1.02	0.01	4.37	0.01	1.08	0.01	0	0
HD 109246	2.5	0.8	5887	19	1.15	0.01	1.07	0.01	4.43	0.01	1.03	0.01	0	0
HD 109749	4.1	0.7	5860	39	1.55	0.02	1.14	0.01	4.32	0.02	1.21	0.02	1	0
HD 111232	11.6	1.5	5650	22	0.67	0.01	0.79	0.01	4.47	0.02	0.85	0.01	0	0
HD 113337	1.5	0.9	6622	71	4.18	0.08	1.38	0.03	4.19	0.03	1.56	0.05	0	0
HD 114386	8.8	2.8	4926	13	0.28	0.01	0.76	0.01	4.58	0.02	0.73	0.01	0	0

Table A.1. continued.

Star	t (Gyr)	Δt (Gyr)	$T_{\rm eff}$ (K)	$\Delta T_{\rm eff}$ (K)	L ($L_\odot$)	ΔL ($L_\odot$)	M ($M_\odot$)	ΔM ($M_\odot$)	$\log g$ (cm/s^2)	$\Delta\log g$ (cm/s^2)	R ($R_\odot$)	ΔR ($R_\odot$)	Bin	Tr
HD 114613	5.0	0.1	5756	13	4.09	0.03	1.25	0.01	3.91	0.01	2.04	0.02	0	0
HD 114729	9.3	0.6	5939	58	2.33	0.02	0.97	0.01	4.1	0.02	1.44	0.03	1	0
HD 114762	12.4	0.6	6043	22	1.52	0.01	0.82	0.01	4.24	0.01	1.13	0.01	1	0
HD 114783	10.4	2.4	5089	17	0.4	0.01	0.81	0.01	4.53	0.02	0.81	0.01	0	0
HD 11506	2.0	0.6	6119	45	2.1	0.1	1.25	0.01	4.31	0.02	1.29	0.04	0	0
HD 116029	4.9	1.1	4849	39	11.4	0.1	1.3	0.1	3.19	0.04	4.8	0.1	0	0
HD 117207	6.6	1.0	5681	33	1.19	0.02	1.03	0.01	4.34	0.02	1.13	0.02	0	0
HD 117618	4.0	1.3	6019	50	1.6	0.1	1.1	0.02	4.34	0.03	1.17	0.04	0	0
HD 118203	5.4	0.5	5741	35	3.8	0.3	1.23	0.03	3.93	0.02	2.0	0.1	0	0
HD 11964	8.5	0.5	5371	43	2.6	0.1	1.09	0.02	3.92	0.02	1.9	0.1	1	0
HD 11977	2.9	0.2	4851	9	62.1	0.2	1.46	0.03	2.5	0.01	11.2	0.1	0	0
HD 120084	4.4	1.2	4675	11	52	1	1.3	0.1	2.48	0.03	11.0	0.2	0	0
HD 121504	1.9	1.0	6089	47	1.62	0.04	1.16	0.02	4.38	0.03	1.15	0.03	0	0
HD 125595	8.0	3.7	4654	22	0.21	0.01	0.74	0.01	4.61	0.02	0.71	0.02	0	0
HD 125612	3.1	0.3	5818	13	1.205	0.003	1.09	0.01	4.4	0.01	1.08	0.01	1	0
HD 12661	3.3	0.6	5714	22	1.13	0.01	1.09	0.01	4.4	0.01	1.08	0.01	0	0
HD 128311	8.5	3.6	4922	26	0.29	0.01	0.77	0.02	4.58	0.02	0.74	0.02	0	0
HD 130322	6.1	2.9	5410	30	0.56	0.01	0.88	0.02	4.52	0.03	0.85	0.02	0	0
HD 131496	4.0	0.7	4838	43	9.9	0.2	1.4	0.1	3.27	0.04	4.5	0.1	0	0
HD 134987	5.4	0.5	5797	23	1.51	0.01	1.09	0.01	4.3	0.01	1.22	0.01	0	0
HD 136418	5.0	1.0	4997	40	6.9	0.1	1.2	0.1	3.43	0.04	3.5	0.1	0	0
HD 137388	7.3	3.8	5183	25	0.46	0.02	0.87	0.03	4.52	0.03	0.85	0.02	1	0
HD 13908	3.9	0.5	6212	38	4.0	0.1	1.28	0.04	4.06	0.02	1.74	0.04	0	0
HD 13931	5.3	1.3	5902	52	1.48	0.03	1.07	0.02	4.33	0.03	1.17	0.03	0	0
HD 139357	7.2	1.8	4454	39	73.5	1.3	1.1	0.1	2.2	0.1	14.4	0.4	0	0
HD 141937	3.2	0.5	5837	14	1.13	0.01	1.06	0.01	4.42	0.01	1.04	0.01	0	0
HD 142	2.8	0.5	6321	67	2.81	0.05	1.25	0.01	4.24	0.03	1.4	0.04	1	0
HD 142245	3.1	0.3	4831	28	13.1	0.2	1.52	0.05	3.19	0.03	5.2	0.1	0	0
HD 142415	1.6	0.6	5869	12	1.16	0.02	1.1	0.01	4.44	0.01	1.04	0.01	0	0
HD 145377	2.9	1.2	5979	46	1.43	0.04	1.11	0.02	4.38	0.03	1.12	0.03	0	0
HD 145457	2.8	0.6	4772	45	41	1	1.5	0.1	2.66	0.05	9.4	0.2	0	0
HD 1461	4.0	0.7	5807	20	1.20	0.01	1.07	0.01	4.39	0.01	1.08	0.01	0	0
HD 147018	7.3	2.0	5526	29	0.78	0.02	0.94	0.02	4.44	0.03	0.97	0.02	0	0
HD 147513	3.4	0.7	5827	21	1.01	0.01	1.02	0.01	4.45	0.01	0.99	0.01	1	0
HD 148156	1.2	0.5	6156	23	1.84	0.03	1.22	0.01	4.36	0.01	1.19	0.02	0	0
HD 148427	4.3	0.6	4993	44	6.2	0.1	1.32	0.05	3.51	0.03	3.3	0.1	0	0
HD 149026	2.9	0.3	6116	44	2.8	0.1	1.302	0.005	4.2	0.02	1.49	0.04	0	1
HD 149143	4.8	0.8	5792	58	2.2	0.1	1.21	0.03	4.17	0.03	1.5	0.1	0	0
HD 1502	3.0	0.3	5006	25	11.5	0.2	1.46	0.04	3.29	0.02	4.5	0.1	0	0
HD 152581	7.2	2.0	4991	45	16.1	0.2	1.0	0.1	3.0	0.1	5.4	0.1	0	0
HD 153950	4.3	0.8	6136	64	2.24	0.03	1.15	0.02	4.25	0.03	1.33	0.04	0	0
HD 154345	4.1	1.2	5557	15	0.62	0.002	0.9	0.01	4.53	0.01	0.85	0.01	0	0
HD 154672	7.1	0.8	5754	51	1.81	0.02	1.09	0.02	4.2	0.03	1.36	0.03	0	0
HD 154857	5.8	0.5	5740	46	4.4	0.3	1.13	0.03	3.83	0.03	2.1	0.1	0	0
HD 155358	1.9	4.5	5966	53	2.11	0.02	1.1	0.1	4.2	0.04	1.36	0.03	0	0
HD 156279	7.4	2.2	5449	31	0.7	0.01	0.93	0.02	4.45	0.03	0.94	0.02	0	0
HD 156411	4.5	0.3	5886	29	5.1	0.3	1.23	0.02	3.85	0.02	2.2	0.1	0	0
HD 156668	10.2	2.8	4857	18	0.27	0.01	0.75	0.01	4.58	0.01	0.73	0.01	0	0
HD 158038	3.2	0.4	4839	29	11.9	0.1	1.5	0.1	3.23	0.03	4.9	0.1	0	0
HD 159243	2.0	0.3	6071	19	1.45	0.05	1.12	0.01	4.4	0.01	1.09	0.03	0	0
HD 159868	6.3	0.5	5583	54	3.8	0.2	1.13	0.03	3.85	0.03	2.1	0.1	0	0
HD 16141	6.5	0.6	5856	60	2.46	0.03	1.13	0.02	4.12	0.03	1.53	0.04	1	0
HD 16175	4.1	0.8	6009	44	3.35	0.02	1.3	0.05	4.09	0.02	1.69	0.03	0	0
HD 162020	3.1	2.7	4807	17	0.22	0.01	0.75	0.01	4.63	0.01	0.68	0.01	0	0
HD 163607	8.3	0.5	5508	15	2.6	0.1	1.1	0.02	3.98	0.01	1.8	0.1	0	0
HD 16417	6.9	0.4	5818	51	2.74	0.01	1.12	0.01	4.06	0.02	1.63	0.03	0	0
HD 164509	3.2	0.8	5860	31	1.31	0.02	1.1	0.01	4.38	0.02	1.11	0.02	0	0
HD 164922	7.9	2.7	5439	38	0.7	0.01	0.93	0.02	4.45	0.03	0.95	0.02	0	0
HD 167042	3.1	0.3	4989	32	10.7	0.1	1.46	0.05	3.31	0.03	4.4	0.1	0	0
HD 168443	10.0	0.3	5646	36	2.08	0.01	1.02	0.01	4.08	0.01	1.51	0.02	0	0
HD 168746	12.0	0.9	5637	26	1.04	0.01	0.9	0.01	4.32	0.01	1.07	0.01	0	0
HD 169830	2.82	0.03	6276	12	4.656	0.003	1.3975	4.0E-4	4.052	0.004	1.83	0.01	0	0
HD 170469	4.7	0.9	5866	54	1.7	0.1	1.14	0.01	4.28	0.03	1.27	0.05	0	0
HD 171028	8.2	1.1	5771	46	3.9	0.5	0.98	0.04	3.84	0.03	2.0	0.2	0	0
HD 171238	4.0	1.2	5570	21	0.774	0.003	0.99	0.01	4.47	0.01	0.95	0.01	0	0

Table A.1. continued.

Star	t (Gyr)	Δt (Gyr)	$T_{\rm eff}$ (K)	$\Delta T_{\rm eff}$ (K)	L ($L_\odot$)	ΔL ($L_\odot$)	M ($M_\odot$)	ΔM ($M_\odot$)	$\log g$ (cm/s^2)	$\Delta\log g$ (cm/s^2)	R ($R_\odot$)	ΔR ($R_\odot$)	Bin	Tr
HD 17156	4.9	0.6	5943	38	2.46	0.05	1.2	0.03	4.17	0.02	1.48	0.03	0	1
HD 173416	1.8	0.7	4790	37	80	2	1.8	0.2	2.5	0.1	13.0	0.3	0	0
HD 175541	2.9	0.2	5093	23	10.0	0.1	1.45	0.03	3.37	0.02	4.07	0.05	0	0
HD 177830	10.2	1.7	4735	31	5.3	0.1	1.1	0.1	3.39	0.04	3.4	0.1	1	0
HD 178911 B	4.8	1.3	5642	29	1.00	0.02	1.03	0.02	4.4	0.02	1.05	0.02	1	0
HD 179079	7.8	0.4	5649	47	2.392	0.004	1.11	0.01	4.06	0.02	1.62	0.03	0	0
HD 179949	1.2	0.6	6220	28	1.95	0.01	1.23	0.01	4.36	0.01	1.2	0.01	0	0
HD 180314	0.9	0.2	4946	55	40	1	2.3	0.1	2.92	0.05	8.7	0.3	0	0
HD 180902	3.3	0.5	5001	44	9.4	0.1	1.4	0.1	3.36	0.04	4.1	0.1	0	0
HD 181342	3.6	0.6	4856	41	12.3	0.4	1.4	0.1	3.2	0.04	5.0	0.2	0	0
HD 181433	7.4	3.4	4909	20	0.34	0.01	0.84	0.02	4.55	0.02	0.8	0.02	0	0
HD 181720	12.4	0.5	5840	49	2.112	0.003	0.87	0.01	4.06	0.02	1.42	0.02	0	0
HD 183263	4.5	0.8	5870	56	1.8	0.1	1.16	0.02	4.28	0.03	1.29	0.05	0	0
HD 185269	4.1	0.5	6023	43	4.5	0.1	1.3	0.04	3.97	0.03	2.0	0.1	1	0
HD 187085	2.7	0.8	6163	53	2.0	0.1	1.19	0.02	4.31	0.03	1.26	0.04	0	0
HD 187123	5.6	1.3	5853	53	1.44	0.02	1.06	0.02	4.32	0.03	1.17	0.03	0	0
HD 18742	3.9	0.8	4956	40	14.0	0.2	1.3	0.1	3.14	0.04	5.1	0.1	0	0
HD 188015	5.9	1.3	5722	52	1.41	0.03	1.08	0.02	4.3	0.03	1.21	0.03	1	0
HD 189733	5.3	3.8	5019	23	0.327	0.003	0.81	0.02	4.58	0.02	0.76	0.01	1	1
HD 190360	7.3	1.6	5628	47	1.12	0.03	1.01	0.02	4.34	0.03	1.12	0.03	1	0
HD 190647	8.7	0.4	5630	48	2.19	0.01	1.07	0.01	4.07	0.02	1.56	0.03	0	0
HD 192263	5.9	3.9	4980	20	0.3	0.01	0.78	0.02	4.59	0.02	0.73	0.01	0	0
HD 192310	8.1	3.2	5153	21	0.4	0.01	0.82	0.02	4.54	0.02	0.79	0.01	0	0
HD 192699	3.1	0.4	5097	36	11.1	0.1	1.39	0.05	3.31	0.03	4.3	0.1	0	0
HD 195019	7.7	0.7	5825	56	2.23	0.02	1.08	0.01	4.13	0.02	1.47	0.04	1	0
HD 196050	5.4	0.7	5884	47	2.09	0.02	1.15	0.02	4.2	0.02	1.4	0.03	1	0
HD 19994	3.1	0.3	6164	62	3.78	0.04	1.35	0.01	4.1	0.02	1.71	0.04	1	0
HD 200964	3.1	0.4	5059	34	12.8	0.2	1.4	0.1	3.23	0.03	4.7	0.1	0	0
HD 202206	2.9	1.0	5719	26	1.04	0.01	1.07	0.02	4.43	0.02	1.04	0.01	0	0
HD 2039	4.4	0.9	5927	60	2.1	0.1	1.19	0.02	4.23	0.04	1.4	0.1	0	0
HD 204313	4.3	1.8	5783	48	1.18	0.03	1.06	0.03	4.39	0.04	1.08	0.03	0	0
HD 204941	3.9	3.3	5072	17	0.297	0.003	0.77	0.02	4.62	0.02	0.71	0.01	1	0
HD 205739	2.9	0.2	6247	40	3.581	0.003	1.335	0.003	4.14	0.01	1.62	0.02	0	0
HD 206610	3.0	0.3	4836	30	18	1	1.51	0.05	3.05	0.03	6.0	0.2	0	0
HD 20782	5.4	1.3	5876	31	1.20	0.03	1.01	0.02	4.39	0.03	1.06	0.03	1	0
HD 207832	1.4	0.8	5676	40	0.82	0.04	1.03	0.02	4.5	0.01	0.94	0.04	0	0
HD 20794	11.6	1.5	5602	20	0.642	0.003	0.8	0.01	4.47	0.02	0.85	0.01	0	0
HD 208487	2.3	0.9	6143	47	1.76	0.05	1.16	0.02	4.36	0.03	1.17	0.03	0	0
HD 20868	8.2	2.7	4769	24	0.25	0.01	0.77	0.01	4.59	0.01	0.73	0.02	0	0
HD 209458	4.4	1.2	6047	62	1.8	0.04	1.11	0.02	4.3	0.04	1.22	0.04	0	1
HD 210277	8.8	1.9	5530	40	0.92	0.03	0.96	0.02	4.37	0.03	1.05	0.03	0	0
HD 210702	3.1	0.3	4946	25	12.9	0.1	1.47	0.04	3.22	0.02	4.9	0.1	0	0
HD 212771	2.9	0.1	5008	14	15.1	0.2	1.45	0.02	3.16	0.02	5.2	0.1	0	0
HD 213240	4.6	0.6	6029	37	2.6	0.1	1.2	0.02	4.17	0.02	1.48	0.03	1	0
HD 215497	9.9	2.8	5128	12	0.47	0.02	0.86	0.02	4.49	0.03	0.87	0.02	0	0
HD 216437	5.2	0.7	5898	37	2.23	0.03	1.17	0.03	4.19	0.02	1.43	0.03	0	0
HD 216770	5.4	2.9	5406	39	0.66	0.01	0.95	0.03	4.48	0.03	0.93	0.02	0	0
HD 217107	4.2	1.0	5676	31	1.14	0.01	1.08	0.01	4.38	0.02	1.11	0.02	0	0
HD 217786	6.8	0.9	6031	55	1.93	0.04	1.03	0.02	4.23	0.03	1.27	0.04	0	0
HD 218566	8.0	3.1	4880	16	0.3	0.01	0.8	0.01	4.57	0.02	0.77	0.02	0	0
HD 219828	5.2	0.8	5921	53	2.74	0.03	1.2	0.04	4.11	0.03	1.58	0.04	0	0
HD 220773	6.3	0.1	5852	26	3.16	0.01	1.154	0.003	4.02	0.01	1.73	0.02	0	0
HD 221287	2.8	0.3	6193	20	2.0	0.1	1.17	0.01	4.33	0.01	1.22	0.03	0	0
HD 222155	8.1	0.4	5814	43	2.9	0.1	1.05	0.01	4.00	0.01	1.7	0.1	0	0
HD 222582	6.2	1.1	5851	32	1.24	0.01	1.01	0.02	4.36	0.02	1.09	0.02	1	0
HD 224693	3.9	0.5	5972	49	4.1	0.1	1.35	0.04	4.01	0.01	1.89	0.05	0	0
HD 22781	7.5	2.9	5152	27	0.32	0.01	0.74	0.02	4.6	0.02	0.71	0.02	0	0
HD 23079	4.1	1.4	6039	44	1.37	0.03	1.03	0.02	4.39	0.03	1.07	0.03	0	0
HD 23127	4.4	0.6	5841	45	3.08	0.02	1.29	0.03	4.07	0.02	1.72	0.03	0	0
HD 231701	3.7	0.5	6211	71	2.94	0.05	1.23	0.01	4.18	0.03	1.48	0.05	0	0
HD 23596	4.0	0.7	5979	68	2.65	0.03	1.25	0.03	4.17	0.03	1.52	0.04	0	0
HD 24040	4.9	0.9	5910	53	1.78	0.05	1.13	0.02	4.27	0.03	1.27	0.04	0	0
HD 25171	4.8	0.9	6131	57	1.94	0.02	1.08	0.02	4.28	0.03	1.24	0.03	0	0
HD 2638	5.1	4.1	5173	26	0.42	0.01	0.87	0.03	4.55	0.03	0.81	0.02	0	0
HD 27894	6.9	4.3	4923	32	0.33	0.01	0.83	0.03	4.56	0.03	0.79	0.02	0	0

Table A.1. continued.

Star	t (Gyr)	Δt (Gyr)	$T_{\rm eff}$ (K)	$\Delta T_{\rm eff}$ (K)	L ($L_\odot$)	ΔL ($L_\odot$)	M ($M_\odot$)	ΔM ($M_\odot$)	$\log g$ (cm/s^2)	$\Delta \log g$ (cm/s^2)	R ($R_\odot$)	ΔR ($R_\odot$)	Bin	Tr
HD 28185	5.5	4.2	5615	56	1.17	0.02	1.0	0.1	4.33	0.03	1.15	0.03	0	0
HD 28254	7.8	0.4	5607	37	2.19	0.01	1.11	0.01	4.08	0.02	1.57	0.02	1	0
HD 28678	6.1	1.7	4798	43	24.0	0.4	1.1	0.1	2.8	0.1	7.1	0.2	0	0
HD 290327	11.5	1.3	5543	13	0.74	0.02	0.85	0.01	4.42	0.02	0.93	0.02	0	0
HD 2952	3.1	0.3	4755	18	61.5	0.4	1.5	0.1	2.47	0.02	11.6	0.1	0	0
HD 30177	5.9	1.1	5596	32	1.09	0.01	1.05	0.01	4.36	0.02	1.11	0.02	0	0
HD 30562	3.7	0.5	6000	55	2.8	0.02	1.28	0.02	4.16	0.02	1.55	0.03	0	0
HD 30856	7.3	1.8	4911	41	10.0	0.2	1.1	0.1	3.19	0.05	4.4	0.1	0	0
HD 31253	4.0	0.7	6105	63	2.9	0.1	1.25	0.04	4.16	0.03	1.5	0.1	0	0
HD 32518	5.8	1.5	4610	40	47	1	1.2	0.1	2.4	0.1	10.8	0.3	0	0
HD 330075	6.1	4.0	5127	26	0.4	0.03	0.84	0.02	4.55	0.03	0.8	0.04	0	0
HD 33142	3.3	0.4	4980	37	10.5	0.2	1.4	0.1	3.31	0.03	4.4	0.1	0	0
HD 33283	3.9	0.6	5980	54	4.43	0.02	1.37	0.04	3.98	0.03	1.97	0.04	0	0
HD 34445	3.7	0.6	6038	53	2.1	0.1	1.19	0.01	4.27	0.03	1.32	0.04	1	0
HD 3651	6.9	2.8	5271	26	0.51	0.01	0.88	0.02	4.51	0.02	0.86	0.01	1	0
HD 37124	11.1	1.7	5733	37	0.81	0.01	0.82	0.02	4.42	0.02	0.92	0.02	0	0
HD 37605	4.2	1.4	5364	25	0.62	0.01	0.96	0.01	4.49	0.01	0.91	0.02	0	0
HD 38283	6.5	0.6	6080	59	2.56	0.01	1.07	0.02	4.14	0.03	1.45	0.03	0	0
HD 38529	3.98	0.03	5526	17	5.81	0.03	1.412	0.003	3.74	0.01	2.64	0.02	1	0
HD 38801	4.8	0.3	5323	52	3.7	0.1	1.28	0.02	3.82	0.02	2.3	0.1	0	0
HD 39091	2.8	0.8	6018	31	1.5	0.02	1.12	0.01	4.37	0.02	1.13	0.02	0	0
HD 40307	6.9	4.0	4956	18	0.243	0.003	0.71	0.02	4.63	0.02	0.67	0.01	0	0
HD 40979	1.5	0.6	6163	25	1.82	0.03	1.21	0.01	4.36	0.02	1.19	0.02	1	0
HD 4113	5.8	1.6	5717	46	1.16	0.04	1.03	0.02	4.36	0.03	1.1	0.03	1	0
HD 4203	7.3	0.9	5640	57	1.71	0.02	1.09	0.02	4.2	0.03	1.37	0.04	0	0
HD 4208	7.4	2.4	5678	33	0.71	0.01	0.86	0.02	4.48	0.03	0.88	0.02	0	0
HD 4308	0.4	2.2	5674	51	1.02	0.03	0.96	0.03	4.37	0.02	1.05	0.03	0	0
HD 4313	3.0	0.3	4920	21	14.0	0.2	1.49	0.04	3.18	0.02	5.2	0.1	0	0
HD 43197	4.4	2.1	5457	33	0.75	0.02	1.00	0.02	4.46	0.03	0.97	0.03	0	0
HD 43691	2.1	1.7	6101	67	3.2	0.1	1.33	0.03	4.14	0.03	1.6	0.1	0	0
HD 44219	9.7	0.8	5739	50	1.82	0.02	1.01	0.01	4.16	0.02	1.37	0.03	0	0
HD 45350	7.1	0.9	5683	35	1.43	0.02	1.06	0.01	4.27	0.02	1.24	0.02	0	0
HD 45364	5.8	2.4	5523	28	0.575	0.004	0.86	0.02	4.53	0.02	0.83	0.01	0	0
HD 45652	5.4	2.7	5342	31	0.61	0.01	0.94	0.02	4.49	0.03	0.91	0.02	0	0
HD 46375	11.9	1.1	5379	19	0.77	0.01	0.91	0.01	4.38	0.01	1.01	0.01	1	0
HD 47186	5.3	0.8	5729	24	1.19	0.02	1.05	0.01	4.36	0.02	1.11	0.02	0	0
HD 49674	3.6	0.8	5655	25	0.99	0.02	1.06	0.01	4.42	0.01	1.04	0.02	0	0
HD 50499	2.3	0.4	6112	30	2.26	0.04	1.27	0.01	4.28	0.02	1.34	0.03	0	0
HD 50554	2.1	0.5	6047	17	1.37	0.01	1.1	0.01	4.41	0.01	1.07	0.01	0	0
HD 52265	2.2	0.7	6183	41	2.06	0.03	1.22	0.01	4.32	0.02	1.25	0.02	0	0
HD 5319	6.1	1.4	4888	39	8.2	0.1	1.2	0.1	3.3	0.04	4.0	0.1	0	0
HD 5608	3.0	0.3	4897	25	13.1	0.3	1.5	0.04	3.2	0.02	5.0	0.1	0	0
HD 5891	5.7	1.5	4796	41	39.1	0.4	1.1	0.1	2.57	0.05	9.1	0.2	0	0
HD 60532	3.0	0.2	6188	17	9.3	0.1	1.46	0.03	3.75	0.02	2.66	0.03	0	0
HD 63454	2.4	3.1	4787	12	0.24	0.01	0.79	0.01	4.62	0.02	0.72	0.01	0	0
HD 63765	7.9	3.1	5474	35	0.58	0.01	0.85	0.02	4.51	0.03	0.85	0.02	0	0
HD 6434	12.2	0.7	5907	21	1.208	0.003	0.83	0.01	4.31	0.01	1.05	0.01	0	0
HD 65216	4.6	3.1	5694	45	0.72	0.02	0.91	0.03	4.51	0.04	0.87	0.02	1	0
HD 66428	5.9	0.8	5721	29	1.28	0.02	1.06	0.01	4.33	0.02	1.15	0.02	0	0
HD 6718	6.2	2.0	5805	46	1.06	0.02	0.97	0.02	4.4	0.03	1.02	0.03	0	0
HD 68988	2.1	0.5	5880	21	1.34	0.02	1.15	0.01	4.39	0.01	1.12	0.02	0	0
HD 69830	10.4	2.5	5401	28	0.59	0.01	0.85	0.02	4.47	0.02	0.88	0.02	0	0
HD 70642	3.6	0.9	5675	18	0.92	0.01	1.02	0.01	4.45	0.01	0.99	0.01	0	0
HD 7199	9.2	2.5	5357	39	0.72	0.01	0.93	0.02	4.41	0.03	0.99	0.02	0	0
HD 72659	6.4	0.7	5994	50	2.09	0.02	1.08	0.02	4.21	0.02	1.34	0.03	0	0
HD 73256	4.5	2.3	5514	35	0.75	0.02	0.98	0.03	4.47	0.03	0.95	0.02	0	0
HD 73267	11.8	1.4	5434	18	0.74	0.01	0.89	0.01	4.4	0.02	0.97	0.01	0	0
HD 73526	7.9	0.5	5669	53	2.18	0.01	1.09	0.01	4.1	0.02	1.53	0.03	0	0
HD 73534	7.1	0.8	4958	45	3.4	0.1	1.15	0.03	3.7	0.03	2.5	0.1	0	0
HD 74156	4.3	0.6	6070	56	3.08	0.03	1.24	0.04	4.12	0.03	1.59	0.04	0	0
HD 7449	2.2	1.3	6060	42	1.26	0.02	1.05	0.02	4.44	0.02	1.02	0.02	1	0
HD 75289	1.7	0.4	6143	25	1.97	0.01	1.23	0.01	4.33	0.01	1.24	0.01	1	0
HD 75898	3.8	0.6	6019	66	2.88	0.02	1.28	0.02	4.15	0.03	1.56	0.04	0	0
HD 76700	6.2	0.9	5706	41	1.73	0.03	1.13	0.02	4.22	0.03	1.35	0.03	0	0
HD 77338	7.8	3.4	5261	29	0.57	0.02	0.91	0.03	4.47	0.04	0.91	0.03	0	0

Table A.1. continued.

Star	t (Gyr)	Δt (Gyr)	$T_{\rm eff}$ (K)	$\Delta T_{\rm eff}$ (K)	L ($L_\odot$)	ΔL ($L_\odot$)	M ($M_\odot$)	ΔM ($M_\odot$)	$\log g$ (cm/s^2)	$\Delta\log g$ (cm/s^2)	R ($R_\odot$)	ΔR ($R_\odot$)	Bin	Tr
HD 7924	5.4	2.6	5218	12	0.36	0.01	0.79	0.01	4.59	0.02	0.74	0.01	0	0
HD 79498	4.2	0.9	5741	20	1.11	0.02	1.05	0.01	4.4	0.02	1.07	0.02	1	0
HD 80606	2.7	0.7	5558	23	0.81	0.02	1.03	0.01	4.47	0.01	0.97	0.02	1	1
HD 81040	3.6	1.5	5678	24	0.79	0.02	0.96	0.02	4.49	0.02	0.92	0.02	0	0
HD 81688	6.3	2.9	4830	64	54	1	1.1	0.2	2.4	0.1	10.5	0.4	0	0
HD 82886	3.3	0.5	5083	38	13.5	0.2	1.3	0.1	3.21	0.04	4.8	0.1	0	0
HD 82943	3.1	0.4	5944	18	1.54	0.02	1.14	0.01	4.35	0.01	1.17	0.02	0	0
HD 83443	5.2	1.9	5458	28	0.76	0.02	0.99	0.02	4.45	0.03	0.98	0.02	0	0
HD 8535	3.3	0.5	6142	34	1.92	0.01	1.15	0.01	4.31	0.02	1.23	0.02	0	0
HD 85390	6.8	2.9	5174	17	0.39	0.01	0.81	0.02	4.56	0.02	0.78	0.01	0	0
HD 85512	8.2	3.0	4530	8	0.138	0.002	0.64	0.01	4.67	0.01	0.6	0.01	0	0
HD 8574	4.4	0.6	6092	56	2.35	0.04	1.17	0.02	4.22	0.03	1.38	0.04	0	0
HD 86081	5.5	0.9	5887	56	2.51	0.02	1.18	0.04	4.14	0.03	1.53	0.03	0	0
HD 86264	0.8	0.2	6616	39	4.02	0.04	1.46	0.01	4.23	0.02	1.53	0.02	0	0
HD 87883	7.5	3.8	4971	22	0.327	0.004	0.81	0.02	4.56	0.02	0.77	0.01	0	0
HD 88133	5.7	0.3	5468	25	3.4	0.1	1.23	0.02	3.9	0.02	2.1	0.1	0	0
HD 89307	4.6	1.7	6011	59	1.34	0.03	1.02	0.03	4.38	0.03	1.07	0.03	0	0
HD 89744	2.5	0.3	6270	54	6.29	0.01	1.49	0.02	3.95	0.02	2.13	0.04	1	0
HD 90156	5.7	1.7	5721	28	0.74	0.01	0.89	0.02	4.49	0.02	0.88	0.01	0	0
HD 92788	4.2	1.1	5788	38	1.28	0.02	1.09	0.02	4.36	0.02	1.13	0.02	0	0
HD 93083	6.2	4.4	5025	21	0.35	0.02	0.83	0.02	4.57	0.03	0.78	0.02	0	0
HD 9446	3.7	2.0	5790	45	1.06	0.03	1.04	0.03	4.43	0.03	1.03	0.03	0	0
HD 95089	3.0	0.2	4952	19	13.0	0.1	1.48	0.04	3.22	0.02	4.9	0.1	0	0
HD 96063	2.9	0.2	5073	19	12.3	0.1	1.42	0.03	3.27	0.01	4.5	0.1	0	0
HD 96127	7.2	2.1	3943	34	516	22	1.0	0.1	1.1	0.1	48.8	1.9	0	0
HD 96167	4.7	0.6	5753	49	3.7	0.2	1.3	0.1	3.97	0.02	1.9	0.1	0	0
HD 97658	9.7	2.8	5211	16	0.35	0.01	0.74	0.01	4.58	0.02	0.73	0.01	0	1
HD 98219	3.2	0.4	4952	31	11.4	0.3	1.5	0.1	3.27	0.03	4.6	0.1	0	0
HD 99109	6.0	3.0	5270	24	0.56	0.02	0.93	0.02	4.49	0.03	0.9	0.03	0	0
HD 99492	8.1	3.2	4917	21	0.33	0.01	0.82	0.02	4.55	0.02	0.79	0.02	1	0
HD 99706	2.9	0.2	4847	17	15.6	0.1	1.53	0.03	3.12	0.02	5.6	0.1	0	0
HIP 14810	7.1	2.1	5570	47	0.99	0.03	1.00	0.02	4.37	0.04	1.07	0.04	0	0
HIP 5158	4.5	3.2	4571	14	0.19	0.01	0.75	0.01	4.63	0.02	0.69	0.02	0	0
HIP 57050	8.8	3.6	3542	2	0.0068	2.0E-4	0.2	0.0	5.05	0.01	0.219	0.003	0	0
HIP 57274	8.9	2.1	4636	35	0.2	0.01	0.72	0.01	4.61	0.01	0.69	0.03	0	0
kappa CrB	3.2	0.4	4899	30	11.8	0.2	1.5	0.1	3.24	0.03	4.8	0.1	0	0
KELT-3	1.8	1.2	6413	55	3.3	0.1	1.3	0.02	4.2	0.01	1.5	0.1	0	1
KELT-6	2.6	2.8	6267	46	3.8	0.6	1.2	0.1	4.1	0.1	1.7	0.1	0	1
Kepler-21	3.7	0.4	6264	60	5.20	0.04	1.31	0.03	3.97	0.02	1.94	0.04	0	1
Kepler-37	3.3	0.6	5630	9	0.559	0.002	0.85	0.01	4.57	0.01	0.787	0.004	0	1
Kepler-68	6.1	0.5	5868	32	1.62	0.03	1.07	0.01	4.28	0.01	1.23	0.03	0	1
mu Ara	5.4	0.7	5817	44	1.78	0.04	1.14	0.02	4.25	0.03	1.32	0.04	0	0
NGC 2423 3	6.7	3.0	4446	26	73	14	1.2	0.2	2.19	0.01	14.4	1.6	0	0
Qatar-1	6.9	3.8	4730	15	0.24	0.01	0.78	0.02	4.59	0.02	0.73	0.01	0	1
tau Boo	1.8	0.4	6408	45	3.11	0.04	1.33	0.01	4.24	0.02	1.43	0.03	1	0
TrES-1	9.5	3.1	5492	57	0.77	0.02	0.91	0.03	4.42	0.04	0.97	0.03	0	1
TrES-2	5.0	1.0	5958	65	1.7	0.1	1.09	0.03	4.3	0.01	1.2	0.1	0	1
TrES-3	7.9	1.4	5614	29	0.77	0.01	0.9	0.02	4.45	0.01	0.93	0.02	0	1
TrES-4	2.1	0.1	6327	25	3.42	0.04	1.37	0.01	4.192	0.004	1.54	0.02	0	1
TrES-5	7.5	3.7	5087	31	0.41	0.01	0.85	0.03	4.53	0.03	0.82	0.02	0	1
WASP-11	5.7	2.1	4917	18	0.29	0.01	0.79	0.01	4.59	0.01	0.74	0.02	0	1
WASP-14	1.5	1.4	6454	52	4.2	0.5	1.33	0.04	4.13	0.03	1.7	0.1	0	1
WASP-16	8.5	1.2	5633	49	1.09	0.04	0.98	0.02	4.34	0.01	1.1	0.04	0	1
WASP-18	0.9	0.2	6167	7	1.7	0.04	1.2	0.001	4.39	0.01	1.15	0.02	0	1
WASP-19	3.6	1.8	5526	39	0.76	0.01	1.00	0.02	4.47	0.02	0.95	0.02	0	1
WASP-2	0.7	0.3	5345	8	0.47	0.01	0.9	0.001	4.581	0.004	0.8	0.01	0	1
WASP-21	3.7	0.7	6123	38	1.43	0.03	1.03	0.02	4.39	0.01	1.06	0.02	0	1
WASP-25	3.2	1.2	5582	21	0.72	0.02	0.97	0.01	4.5	0.01	0.91	0.02	0	1
WASP-26	3.1	0.4	5881	13	1.26	0.01	1.09	0.01	4.4	0.01	1.08	0.01	0	1
WASP-34	6.8	1.3	5758	55	1.19	0.03	1.01	0.02	4.35	0.02	1.1	0.04	0	1
WASP-37	7.7	1.4	5956	55	1.1	0.04	0.9	0.02	4.39	0.02	0.99	0.04	0	1
WASP-39	6.7	2.4	5466	34	0.57	0.01	0.86	0.02	4.51	0.02	0.85	0.01	0	1
WASP-4	5.5	2.0	5435	31	0.6	0.01	0.91	0.02	4.51	0.02	0.88	0.01	0	1
WASP-41	3.9	1.0	5555	27	0.7	0.02	0.96	0.01	4.5	0.01	0.91	0.02	0	1
WASP-43	2.4	2.3	4756	12	0.215	0.002	0.75	0.01	4.64	0.01	0.68	0.01	0	1

Table A.1. continued.

Star	t (Gyr)	Δt (Gyr)	$T_{\rm eff}$ (K)	$\Delta T_{\rm eff}$ (K)	L ($L_\odot$)	ΔL ($L_\odot$)	M ($M_\odot$)	ΔM ($M_\odot$)	$\log g$ (cm/s^2)	$\Delta \log g$ (cm/s^2)	R ($R_\odot$)	ΔR ($R_\odot$)	Bin	Tr
WASP-44	6.8	2.8	5402	31	0.6	0.02	0.9	0.02	4.49	0.03	0.89	0.02	0	1
WASP-48	9.1	0.8	5770	53	2.6	0.2	1.01	0.02	4.03	0.01	1.6	0.1	0	1
WASP-5	2.5	0.7	5611	14	0.79	0.02	1.01	0.01	4.49	0.01	0.94	0.01	0	1
WASP-52	3.8	2.6	5077	14	0.348	0.004	0.83	0.02	4.58	0.02	0.76	0.01	0	1
WASP-54	3.3	0.4	6090	26	1.61	0.02	1.1	0.01	4.36	0.01	1.14	0.02	0	1
WASP-58	12.6	0.1	5874	5	1.23	0.01	0.839	0.002	4.2936	1.0E-4	1.073	0.005	0	1
WASP-60	8.8	1.4	5730	52	1.09	0.03	0.95	0.02	4.36	0.02	1.06	0.04	0	1
WASP-75	2.9	0.2	5862	9	1.1	0.01	1.051	0.004	4.435	0.002	1.02	0.01	0	1
WASP-8	4.2	1.1	5632	34	0.96	0.02	1.04	0.02	4.42	0.01	1.03	0.02	1	1
XO-2	9.6	0.9	5474	54	1.7	0.1	1.04	0.03	4.13	0.01	1.4	0.1	1	1
XO-3	1.7	1.0	6685	45	3.7	0.1	1.26	0.01	4.22	0.01	1.43	0.04	0	1
XO-5	12.4	0.6	5452	12	0.794	0.004	0.89	0.01	4.38	0.01	1.00	0.01	0	1